UNIVERSITÄT AUGSBURG
Universitätsbibliothek

OPEN ACCESS
OPUS AUGSBURG

Zr(IV) and Ce(IV)-based metal-organic frameworks incorporating 4-carboxycinnamic acid as ligand: synthesis and properties

Mostakim SK, Maciej Grzywa, Dirk Volkmer, Shyam Biswas

Angaben zur Veröffentlichung / Publication details:

SK, Mostakim, Maciej Grzywa, Dirk Volkmer, and Shyam Biswas. 2017. "Zr(IV) and Ce(IV)-based metal-organic frameworks incorporating 4-carboxycinnamic acid as ligand: synthesis and properties." *Microporous and Mesoporous Materials* 237: 275–81. https://doi.org/10.1016/j.micromeso.2016.09.034.

Nutzungsbedingungen / Terms of use:

CC BY-NC-ND 4.0

Dieses Dokument wird unter folgenden Bedingungen zur Verfügung gestellt: / This document is made available under these conditions:
CC-BY-NC-ND 4.0: Creative Commons: Namensnennung - Nicht kommerziell - Keine Bearbeitung
Weitere Informationen finden Sie unter: / For more information see:
https://creativecommons.org/licenses/by-nc-nd/4.0/deed.de

Zr(IV) and Ce(IV)-based metal-organic frameworks incorporating 4-carboxycinnamic acid as ligand: Synthesis and properties

Mostakim SK [a], Maciej Grzywa [b], Dirk Volkmer [b], Shyam Biswas [a, *]

[a] Department of Chemistry, Indian Institute of Technology Guwahati, 781039 Assam, India
[b] Institute of Physics, Chair of Solid State Science, Augsburg University, Universitätsstrasse 1, 86135 Augsburg, Germany

1. Introduction

In the last two decades, research activities on metal-organic frameworks (MOFs) [1–5] have grown exponentially. This is due to their potential applications in a wide range of areas such as gas storage/separation [6–10], heterogeneous catalysis [11–13], chemical sensing [14–19], drug delivery [20–22] and polymerization [23]. MOFs are a new class of highly crystalline and porous materials. They are built up of inorganic building blocks. The interconnection of the inorganic building units by polytopic organic ligand molecules results in 3D framework structures having well-defined pore systems (channels, cages, etc.). Since an almost infinite combination of metal ions and organic ligands are possible, a huge variety of porous MOF structures have been reported until today. It is possible to tune the pore dimensions (hence specific surface area and pore volume) and pore surface characteristics of MOFs by varying the sizes [24] of the organic ligands and by grafting various functional groups [25–30] to the organic ligands, respectively. However, such modifications of the pore systems are not feasible for traditional porous adsorbents such as zeolites, mesoporous silicas and activated carbons. Owing to their modular nature, a great deal of research have been devoted to the design and synthesis of new porous MOFs for accomplishing a target application.

MOF materials having high physicochemical stability (air, water, thermal, acid-base, etc.) are highly desirable for their applications in industry. Several famous MOF compounds [31–35] have shown low physicochemical stability and therefore they are not suitable for industrial applications, although they have displayed great potential [10,36–40] for gas adsorption and separation. The employment of transition metal ions with high oxidation states (such as, Ti(IV) [41], Zr(IV) [42], Hf(IV) [43], etc.) is one of the approaches for synthesizing MOF materials having relatively higher physicochemical stability. Among numerous Zr(IV)-based MOF materials reported till date [44–46], the microporous UiO-66 (UiO = University of Oslo) compound [42] has attracted the attention of researchers owing to its high thermal and chemical stability as well as promising performances for CO_2/CH_4 separation [47,48]. The three-dimensional (3D) cubic framework of this MOF material is constructed from $[Zr_6O_4(OH)_4]^{12+}$ building units which are interconnected by 1,4-benzenedicarboxylate (BDC) ligands. The use of longer 2,6-naphthalenedicarboxylate (NDC) ligand instead of BDC resulted in the formation of Zr(IV) and Hf(IV)-based DUT-52 (DUT = Dresden University of Technology) [43] framework compounds, which possess the same framework topology as that of UiO-66. Zr-DUT-52 material has been also termed as Zr-NDC [49]

* Corresponding author.
E-mail address: sbiswas@iitg.ernet.in (S. Biswas).

and Zr_6-NDC [50] in other reports. This MOF compound also exhibits high physicochemical stability and significant microporosity like UiO-66. The presented Zr(IV) (**1**) and Ce(IV) (**2**) based MOF compounds consisting of 4-carboxycinnamate (CCA) ligands (Scheme 1) are isostructural with DUT-52 and hence both of them bear UiO-66 framework topology. It is noteworthy that, only a handful examples of Ce(IV)-based MOF compounds have been reported till date. Very recently, the synthesis, properties and redox catalytic activities of nine Ce(IV)-based MOF materials with UiO-66 structures containing ligands of different sizes and functionalities have been reported by Stock et al. [51] More recently, we have employed the Ce(IV)-based azide and nitro-functionalized UiO-66 materials as turn-on fluorescence probes for the sensing of H_2S [52]. Although the CCA ligand has been formerly employed for the construction of few MOFs with divalent metal ions [53–59], it has never been incorporated into MOFs having tetravalent metal ions such as Zr(IV) and Ce(IV). Therefore, we hypothesized that the employment of the CCA ligand and tetravalent metal ions would give rise to MOFs having high physicochemical stability. In this report, we present the synthesis, complete characterization, thermal and chemical stability as well as gas sorption behavior of the new Zr(IV) (**1**) and Ce(IV) (**2**) based MOF compounds containing the CCA ligand.

2. Experimental

2.1. Materials and general methods

The H_2CCA ligand was synthesized according to a previously published procedure [56]. All other starting materials were of reagent grade and used as received from the commercial suppliers. Fourier transform infrared (FT-IR) spectra were recorded in the region of 440–4000 cm^{-1} with a Perkin Elmer Spectrum Two FT-IR spectrometer. The following indications are used to characterize absorption bands: very strong (vs), strong (s), medium (m), weak (w), shoulder (sh), and broad (br). Elemental analyses (C, H, N) were carried out on a Thermo Scientific Flash 2000 CHNSO analyzer equipped with a TCD detector. Thermogravimetric analyses (TGA) were performed with a Mettler-Toledo TGA/SDTA 851e thermogravimetric analyzer in a temperature range of 30–600 °C under air atmosphere at a heating rate of 5 °C min^{-1}. Ambient temperature X-Ray powder diffraction (XRPD) patterns were recorded on a Bruker D2 Phaser X-ray diffractometer (30 kV, 10 mA) or a Bruker D8 Advance θ-2θ diffractometer (40 kV, 40 mA) in transmittance Bragg-Brentano geometry equipped with a LYNXEYE 1D detector and Göbel mirror, using Cu-Kα ($\lambda = 1.5406$ Å) radiation. Le Bail fits of the XRD patterns of as-synthesized **1** and **2** were performed by using the Jana2006 program [60]. The solution ^{1}H-NMR spectra were recorded on a Bruker AM 300 spectrometer at 300 MHz. Before the NMR measurements, the compounds (20 mg each) were digested in 500 μL of 1 M NaOH in D_2O for 24 h. The nitrogen sorption isotherms up to 1 bar were measured using a Quantachrome Autosorb iQ-MP gas sorption analyzer at −196 °C. The carbon dioxide adsorption measurements were performed using a Quantachrome iSorb-HP gas sorption analyzer at 0 °C. Prior to the sorption experiments, the samples of **1** and **2** were degassed by heating (190° C, 6 h for **1**; 50 °C, 4 h for **2**) under dynamic vacuum.

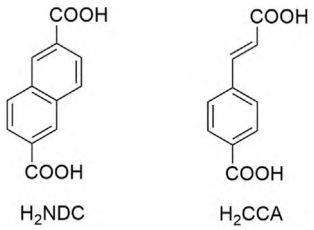

Scheme 1. (a) Structure of the H_2NDC ligand used previously for the synthesis of DUT-52 framework. (b) Structure of the H_2CCA ligand used in this work for the synthesis of **1** and **2**.

The lattice models of **1** and **2** were constructed by transforming the crystallographic unit cell of UiO-66 [42] from space group $F\bar{4}3m$ into P23. The latter setting allowed us to transform the H_2BDC ligand into the less symmetric H_2CCA ligand while retaining a cubic crystal system. Both lattice models were fully geometry optimized by force-field calculations employing the UFF force field provided in the Forcite module of BIOVIA Materials Studio V8.0 (Accelrys Software, Inc., San Diego, CA, USA) software package. Materials Studio contains a full implementation of the Universal force field, including bond order assignment. The Materials Studio implementation has been rigorously tested and results are in agreement with published work on this force field [61–64]. Once fully relaxed lattice models were obtained, the lattice constants of both compounds were adjusted to the values as given in Table 1 and a constrained geometry optimization was performed to yield the final structural parameters which are given in the Supporting Information.

2.2. Synthesis

Synthesis of $[Zr_6O_4(OH)_4(C_{10}H_6O_4)_6]\cdot 1.5DMF\cdot 17H_2O$ (as-synthesized **1**): A mixture of $ZrCl_4$ (100 mg, 0.43 mmol), H_2CCA ligand (82 mg, 0.43 mmol) and acetic acid (0.25 mL, 4.37 mmol) in 2 mL of DMF was heated in a sealed glass tube at 150 °C for 24 h using an aluminum block heater. After spontaneous cooling to room temperature, the white precipitate was collected by filtration, washed with acetone (4 × 2 mL) and dried in air. The yield was 137 mg (0.06 mmol, 83%) based on the Zr salt. Anal. calcd for $C_{64.5}H_{84.5}N_{1.5}O_{50.5}Zr_6$: C, 34.64 H, 3.80 N, 0.93. Found: C, 34.31 H, 3.74 N, 0.76%. FT-IR (KBr, cm^{-1}): 3418 (br), 1692 (s), 1640 (s), 1588 (s), 1532 (s), 1410 (vs), 1289 (w), 1254 (m), 1208 (w), 1180 (w), 1145 (w), 1111 (w), 1018 (w), 978 (m), 857 (m), 783 (s), 725 (sh), 662 (s), 570 (w), 472 (s).

Synthesis of $[Ce_6O_4(OH)_4(C_{10}H_6O_4)_6]\cdot 6DMF\cdot 16H_2O$ (as-synthesized **2**): A mixture of H_2CCA ligand (40 mg, 0.21 mmol) in DMF (2 mL) and an aqueous solution of ammonium cerium(IV) nitrate (400 μL, 0.5333 M) was sealed in a glass tube and heated using an oil bath under magnetic stirring at 100 °C for 20 min. The yellow precipitate was collected by centrifugation, washed with acetone (4 × 2 mL) and dried in air. The yield was 35 mg (0.02 mmol, 78%) based on the Ce salt. Anal. calcd for $C_{78}H_{114}Ce_6N_6O_{54}$: C, 32.98 H, 4.04 N, 2.95. Found: C, 32.71 H, 4.27 N, 2.75%. FT-IR (KBr, cm^{-1}): 3363 (br), 1647 (vs), 1586 (s), 1536 (s), 1388 (vs), 1288 (w), 1255 (w), 1205 (w), 1183 (w), 1144 (w), 1106 (m), 1012 (sh), 984 (m), 863 (m), 786 (m), 714 (m), 681 (w), 659 (w), 582 (s), 537 (sh), 454 (w).

2.3. Activation of the as-synthesized *1* and *2*

For activation, the as-synthesized sample of **1** was directly heated at 190 °C under vacuum for 6 h. In order to activate **2**, the

Table 1
Refined lattice parameters for as-synthesized **1** and **2** having cubic unit cells.

Compound	*a* (Å)	*V* (Å^3)
1 (as-synthesized)	23.809 (2)	13497 (1)
2 (as-synthesized)	24.6349 (8)	14950.3 (5)
Zr-DUT-52 [43]	23.910 (3)	13669 (3)
Hf-DUT-52 [43]	23.74391 (24)	13395.6 (2)
Zr-NDC [49]	23.7853	–
Zr_6-NDC [50]	23.808 (1)	13495 (2)

as-synthesized form of the compound was stirred in acetone at room temperature for 3 h, during which period, the solvent was discarded and fresh acetone was added after each 1 h. In the second step, the acetone-exchanged form of the compound was heated at 50 °C under vacuum for 4 h. The thermally activated forms of **1** and **2** are denoted as **1′** and **2′**, respectively.

3. Results and discussion

3.1. Synthesis and activation

2 was synthesized by using similar synthesis conditions as described recently for several Ce(IV)-based MOF materials [51,52]. For optimizing the synthesis conditions of **1**, reactions were performed using mixtures of Zr(IV) salts ($ZrCl_4$, $ZrO(NO_3)_2 \cdot xH_2O$ or $ZrOCl_2 \cdot 8H_2O$) and H_2CCA ligand in amide solvents like DMF, *N,N′*-diethylformamide (DEF) or *N,N′*-dimethylacetamide (DMA). Various modulators/additives [65] (benzoic acid, formic acid, acetic acid, trifluoroacetic acid, H_2O or conc. HCl) were added in the reaction mixtures in order to enhance the crystallinity of the compound. All possible combinations (Figs. S1–S3, Supporting Information) of the reactants were employed in these reactions. **1** was obtained with high crystallinity (Fig. S4, Supporting Information) by using $ZrCl_4$ as the metal source and acetic acid as the modulator in DMF. For this combination, $ZrCl_4/H_2CCA$ ligand/acetic acid molar ratio of 1:1:10 was used. Reactions with all other combinations of reactants led to either amorphous products or products having lower crystallinity than **1** with optimum crystallinity. For investigating the effect of varying the $ZrCl_4$/acetic acid ratio on the crystallinity and phase-purity of **1**, various $ZrCl_4$/acetic acid molar ratios ranging from 1:10 to 1:100 were employed (Fig. S4, Supporting Information). **1** was obtained with high crystallinity and phase-purity when $ZrCl_4$/acetic acid molar ratio was 1:10. With increase in the $ZrCl_4$/acetic acid molar ratio, either the crystallinity of the compound decreased or additional peaks in the XRPD patterns due to an unknown crystalline phase were observed.

The physisorbed DMF molecules from the external surface of the as-synthesized samples of **1** and **2** were removed by washing the samples with acetone after filtration. After that, **1** was directly heated under vacuum in order to remove the occluded molecules encapsulated inside the pores. For activating **2**, a two-step procedure was employed. At first, the as-synthesized form of **2** was stirred in acetone for exchanging the guest molecules entrapped within the pores with more volatile acetone molecules. In the second step, the acetone-exchanged form of **2** was heated under vacuum for removing the acetone molecules from the pores. The thermally activated compounds exhibit similar XRPD patterns (Figs. S5 and S6, Supporting Information) as those of the as-synthesized compounds. Therefore, both compounds retain their structural integrity after thermal activation.

3.2. Infrared spectroscopy

The FT-IR spectra of the as-synthesized and thermally activated samples of **1** and **2** (Figs. S7 and S8, Supporting Information) reveal strong absorption bands at around 1590 and 1390 cm^{-1}, which can be attributed to the asymmetric and symmetric $-CO_2$ stretching vibrations of the coordinated CCA ligand molecules, respectively [25–30]. In the IR spectrum of the as-synthesized and activated **1** and **2**, the strong absorption bands observed at around 1640 cm^{-1}

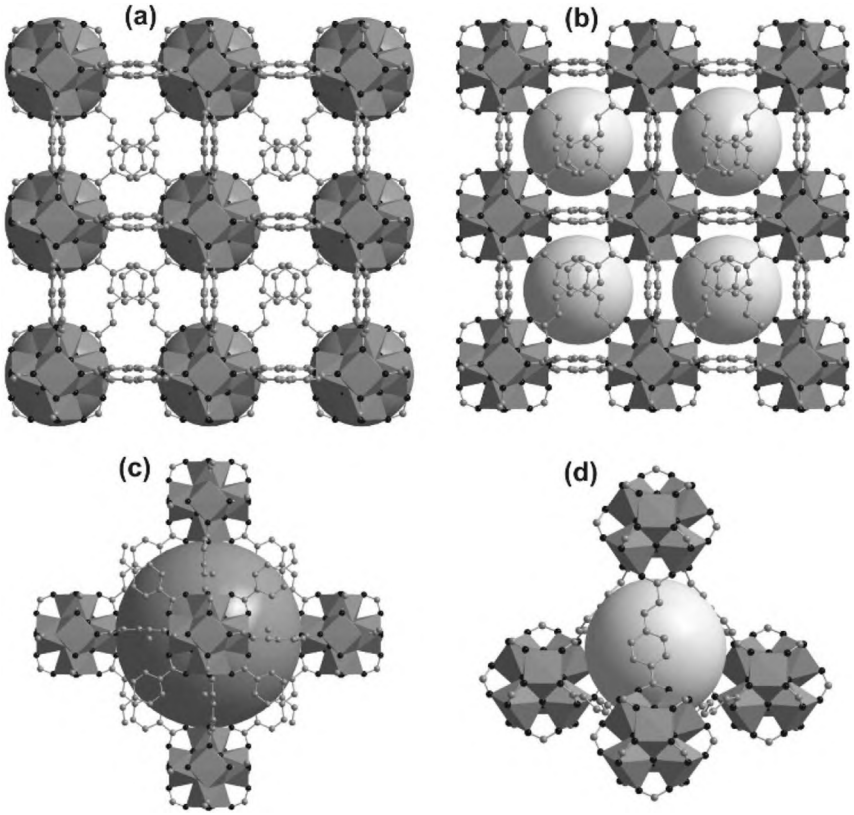

Fig. 1. (a,b) Ball-and-stick representation of the 3D cubic structures of **1** and **2** showing arrangements of the octahedral (dark grey spheres) and tetrahedral (light grey spheres) cages in the framework. (c,d) Enlarged representation of the octahedral and tetrahedral cages. Zr and Ce atoms are shown as polyhedra (color codes: Zr/Ce and C, dark grey; O, black). The hydrogen atoms and occluded molecules have been omitted for clarity.

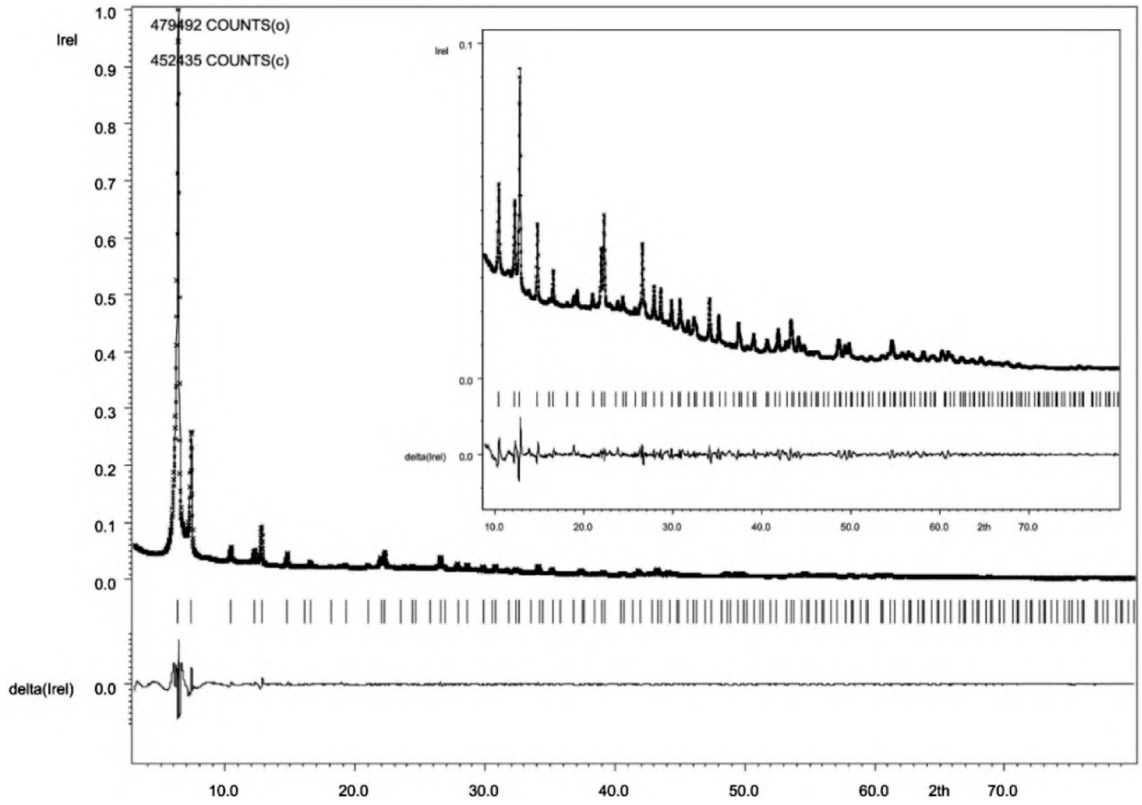

Fig. 2. Le Bail fit of the XRPD pattern of as-synthesized **1**. Dotted and solid lines denote observed and calculated patterns, respectively. The peak markers and the difference plot are displayed at the bottom. Rp = 5.51, Rwp = 7.82.

can be ascribed to the C═C stretching vibration of the coordinated CCA ligand molecules [66]. The strong absorption band at around 1690 cm^{-1} in the IR spectrum of as-synthesized **1** can be attributed to the C═O stretching vibration of the occluded DMF molecules.

3.3. Structure description

Determination of the lattice parameters of the as-synthesized samples of **1** and **2** were carried out from their XRPD patterns measured at ambient conditions. The lattice parameters displayed in Table 1 clearly indicate that both compounds possess cubic structures. The values of the unit cell parameters of the present compounds are close to those of the formerly reported, structurally related DUT-52 framework material [43,49,50,67]. Le Bail fits of the experimental XRPD patterns of as-synthesized **1** and **2** are presented as Figs. 2 and 3, respectively. Good reliability factors were obtained from the fits, which indicated that the experimental XRPD patterns matched well with the calculated ones. The similarity between the theoretical and experimental XRPD patterns for both compounds (Figs. S9 and S10, Supporting Information) confirms their phase-purity. Since the frameworks of **1** and **2** are isostructural with DUT-52 [43,49,50,67], the framework structures (Fig. 1) of the hydroxylated forms of the present compounds are composed of $[M_6O_4(OH)_4]^{12+}$ (M = Zr for **1** or Ce for **2**) building units. In these building units, the μ_3-O and μ_3-OH groups alternatively cap the triangular faces of the M_6 octahedron. The cross-linking of the $[M_6O_4(OH)_4]^{12+}$ building blocks by the carboxylate groups of 12 CCA ligand molecules leads to the formation of cubic, 3D frameworks. In these network structures, both octahedral and tetrahedral shaped microporous cages exist. Each Zr or Ce atom adopts a square-antiprismatic geometry, coordinating with eight O atoms. Four O atoms from carboxylate groups occupy the corners of one square face of the square antiprism, whereas the O atoms from the μ_3-O and μ_3-OH groups are located at the corners of the second square face. In the network structures, every octahedral cage (free diameter ~14 Å) at the center is linked with eight tetrahedral cages (free diameter ~11 Å) at the corners through narrow trigonal windows (free diameter ~8 Å) [49].

3.4. Thermal stability

The thermal stability of the compounds was determined by performing thermogravimetric analyses (TGA) with the as-synthesized as well as activated samples of **1** and **2** in an air atmosphere. The TG analyses (Fig. 4) reveal that **1** and **2** are thermally stable up to 390 and 300 °C, respectively. The high thermal stability of **1** is comparable with those of Zr-UiO-66 and several other Zr(IV)-based MOF materials [27,28,44–46,68–70]. Similarly, the lower thermal stability of **2** than **1** compares well with those of Ce-UiO-66 and few other Ce(IV)-based MOF compounds [51,52].

In the TG traces of as-synthesized **1** and **2** (Fig. 4), the first weight loss steps of 13.5 and 10.5 wt% in the temperature range of 40–130 °C can be ascribed to the removal of 17 and 16 uncoordinated H_2O molecules per formula unit (calcd: 13.6 wt%, **1**; 10.1 wt%, **2**), respectively. The second weight loss steps of 5.0 and 16.0 wt% in the temperature ranges of 130–280 and 130–230 °C can be assigned to the removal of 1.5 and 6 occluded DMF molecules per formula unit of **1** and **2** (calcd: 4.9 wt%, **1**; 15.4 wt%, **2**), respectively. Owing to the removal of organic linker molecules from the framework, the decomposition of **1** and **2** occurs above 390 and 300 °C, respectively. The details of the calculated and experimental weight losses involved with the TG traces of as-synthesized **1** and **2** are presented as Figs. S11–S12 and Table S1, Supporting Information.

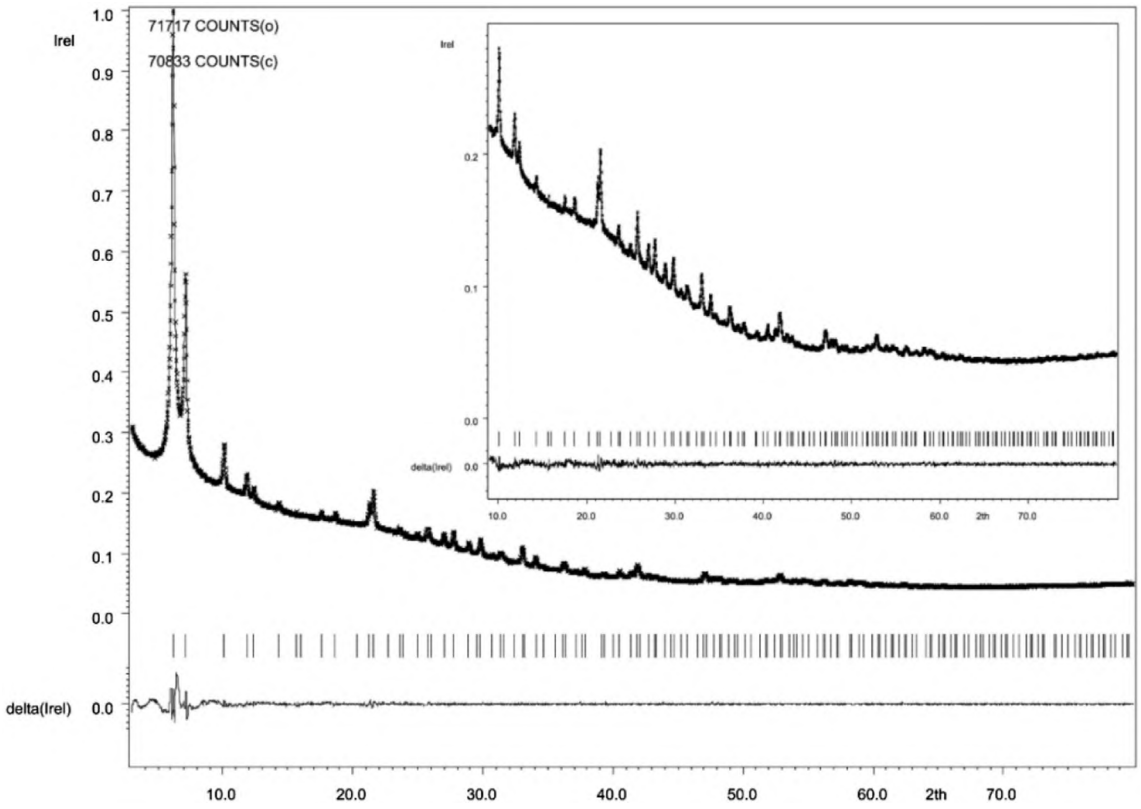

Fig. 3. Le Bail fit of the XRPD pattern of as-synthesized **2**. Dotted and solid lines denote observed and calculated patterns, respectively. The peak markers and the difference plot are displayed at the bottom. Rp = 1.33, Rwp = 1.97.

In the TG curves of **1**′ and **2**′, the first weight loss step can be ascribed to the removal of the adsorbed water molecules. The occurrence of this weight loss step can be related to the exposure of the compounds to air after thermal activation, resulting in hydration of the materials.

The MOFs possessing UiO-66 framework topology exhibit high thermal and chemical stability, although their structures often feature ligand defects [71–74] (generated especially under mild synthesis conditions). The presence of these ligand defects in the structures has been previously shown to affect the porosity of the MOF materials [71,73]. According to the theoretical method described by Lillerud and co-workers [71,73,74], the number of ligand defects has been calculated from the TGA data of thermally activated **1** and **2**. From the TG curve of **1**′, the number of ligand defects per Zr_6 formula unit has been calculated to be 0.95 (Fig. S13, Supporting Information). By applying the same method, no ligand deficiency has been found for **2**′.

3.5. Chemical stability

For determination of the chemical stability of the thermally activated samples (0.05 g for each) of **1** and **2**, the samples were stirred in water, methanol, acetic acid and 1 M HCl solutions (10 mL for each) under ambient conditions for 12 h. After collecting the samples by filtration, the crystallinity of the filtered solids were examined by XRPD measurements (Figs. S5 and S6, Supporting Information). **1**′ retained its crystallinity (and hence structural integrity) after treatment with methanol. The crystallinity of **1**′ was reduced slightly after treatment with water and acetic acid. However, the treatment of **1**′ with 1 M HCl solution lead to substantial reduction in crystallinity. In case of **2**′, the crystallinity was greatly reduced after treatment with methanol and water. The crystallinity of **2**′ was completely lost when treated with acetic acid and 1 M HCl solutions. Therefore, **1**′ exhibited relatively lower chemical stability compared to several other Zr(IV)-based MOF materials [27,28,44–46,68,69]. On the other hand, the low chemical stability of **2**′ is comparable with few other recently reported Ce(IV)-based MOF compounds [51,52].

3.6. Gas adsorption properties

In order to verify the permanent microporosity of the framework materials, N_2 sorption measurements were performed with

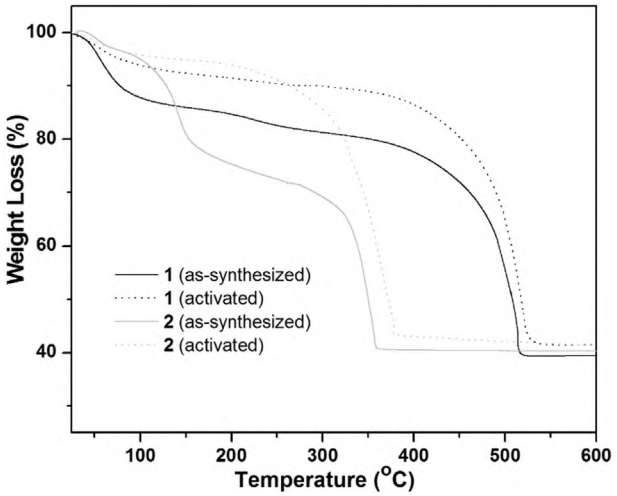

Fig. 4. TG curves of the different forms of **1** and **2** measured in an air atmosphere in the temperature range of 30–600 °C.

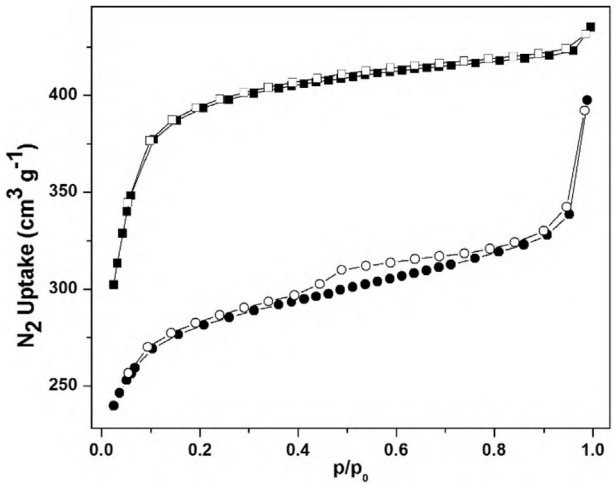

Fig. 5. N_2 adsorption (filled symbols) and desorption (empty symbols) isotherms of **1′** (circles) and **2′** (squares) measured at −196 °C.

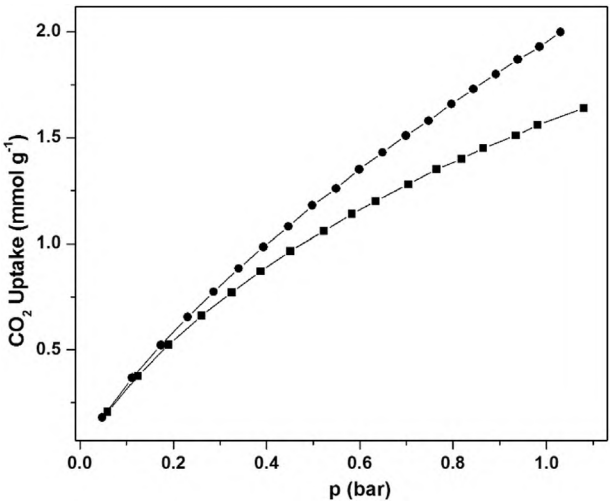

Fig. 6. Low-pressure CO_2 adsorption isotherms of **1′** (circles) and **2′** (squares) recorded at 0 °C.

1′ and **2′**. As displayed in Fig. 5, the adsorption isotherms of the compounds followed type-I behavior. From the N_2 adsorption isotherms, the specific BET surface areas and micropore volumes of the materials were calculated. The specific BET surface areas and micropore volumes of **1′** and **2′** are summarized in Table 2 and Table S2, Supporting Information. The BET surface area and micropore volume of **2′** are comparable with the structurally related Zr(IV) and Hf(IV)-based DUT-52 compounds, although these values are much lower compared to the isostructural Zr-NDC material. On the other side, the BET surface area and micropore volume of **1′** are lower compared to **2′**. This fact can be attributed to the difficulty in activating the as-synthesized sample of **1** by the two-step procedure which has been applied for activating the as-synthesized **2** (i.e., solvent-exchange followed by heating under vacuum).

The accessible surface areas of **1′** and **2′** have been calculated by using the Poreblazer software [75]. The accessible surface areas of **1′** and **2′** have been estimated to be 1421 and 1242 $m^2\ g^{-1}$, respectively. On the other hand, the experimental BET surface areas of **1′** and **2′** are 870 and 1210 $m^2\ g^{-1}$, respectively. Thus, the theoretical surface area of **2′** is close to the experimental value, which supports the structural model of this compound. Since **1′** and **2′** are isostructural, they are expected to show similar experimental surface areas. The lower experimental surface area of **1′** as compared to the theoretical value suggests the incomplete activation of the compound.

In order to check the efficiency of the activation processes, the activated samples of **1** and **2** were digested in 1 M NaOH in D_2O and solution ^1H NMR spectra (Figs. S14–16, Supporting Information) were measured. In addition to the strong peaks due to the CCA ligands, the NMR spectra of **1′** and **2′** contain few weak peaks. Among them, the peaks at δ values of 8.25 and 2.04 ppm can be assigned to formate ion and dimethylamine formed from the decomposition of DMF molecules, respectively [71]. Although we are unable to detect the guest DMF molecules by IR spectroscopy, the existence of their decomposed products (i.e., formate ion and dimethylamine) is visible in the NMR spectra of the two activated compounds. Therefore, the lower specific surface area of the two compounds as compared to the theoretical values can be attributed to the incomplete activation of the compounds (i.e., the presence of guest DMF molecules in the activated compounds).

Table 2
Specific BET surface areas[a] and micropore volumes[b] of **1′** and **2′** determined from the N_2 adsorption isotherms.

Compound	BET surface area ($m^2\ g^{-1}$)	Micropore volume ($cm^3\ g^{-1}$)
1′	870	0.62
2′	1210	0.67
Zr-DUT-52 [43]	1399	0.60
Hf-DUT-52 [43]	1097	0.47
Zr-NDC [49]	1720	0.67
Zr_6-NDC [50]	1287	0.54

[a] Specific BET surface areas were estimated in the p/p_0 range of 0.05–0.1.
[b] Micropore volumes were determined at $p/p_0 = 0.99$.

The permanent microporosity of the framework structures of **1′** and **2′** was also verified by low-pressure CO_2 adsorption measurements at 0 °C. The occurrence of type-I adsorption isotherms (Fig. 6) confirmed microporous nature of both compounds. The CO_2 adsorption capacities of **1′** and **2′** at 0 °C and 1 bar reached 2.0 and 1.6 mmol g^{-1}, respectively. These CO_2 uptake values are comparable with that of the isostructural DUT-52 material [67].

4. Conclusions

We have presented the synthesis, complete characterization, thermal and chemical stability as well as gas sorption characteristics of new Zr(IV) and Ce(IV)-based MOF materials consisting of H_2CCA ligand. Both compounds have been synthesized under solvothermal conditions (150 °C, 24 h for **1**; 100 °C, 20 min for **2**). The phase purity of the compounds were examined by a combination of XRPD analysis, FT-IR spectroscopy, themogravimetric and elemental analyses. As confirmed by the XRPD measurements, both compounds are isostructural with DUT-52 framework material. Based on the thermogravimetric analyses, **1** and **2** are thermally stability up to 390 and 300 °C in air atmosphere, respectively. As revealed from the XRPD experiments, both materials display moderate stability in water and methanol, however they lose their crystallinity when exposed to 1 M HCl. N_2 sorption analyses indicate that **1′** and **2′** exhibit specific BET surface areas of 870 and 1210 $m^2\ g^{-1}$, respectively. The CO_2 uptake values of **1′** and **2′** at 0 °C and 1 bar correspond to 2.0 and 1.6 mmol g^{-1}, respectively.

Acknowledgments

The authors acknowledge financial support from Science and Engineering Research Board (SERB), New Delhi (grant no.

SB/FT/CS-070/2013) and analytical facility from Central Instruments Facility (CIF), IIT Guwahati. We thank Ministry of Human Resource Development for Center of Excellence in FAST (F. No. 5-7/2014-TS-VII).

Appendix A. Supplementary data

Supplementary data related to this article can be found at http://dx.doi.org/10.1016/j.micromeso.2016.09.034.

References

[1] Themed issue on MOFs, Chem. Soc. Rev. 38 (2009) 1201–1508.
[2] Special issue on MOFs, Chem. Rev. 112 (2012) 673–1268.
[3] O.M. Yaghi, M. O'Keeffe, N.W. Ockwig, H.K. Chae, M. Eddaoudi, J. Kim, Nature 423 (2003) 705–714.
[4] G. Férey, Chem. Soc. Rev. 37 (2008) 191–214.
[5] S. Kitagawa, R. Kitaura, S.S. Noro, Angew. Chem. Int. Ed. 43 (2004) 2334–2375.
[6] R. Banerjee, H. Furukawa, D. Britt, C. Knobler, M. O'Keeffe, O.M. Yaghi, J. Am. Chem. Soc. 131 (2009) 3875–3877.
[7] S. Couck, E. Gobechiya, C.E.A. Kirschhock, P.S. Crespo, J.J. AlcaÇiz, A.M. Joaristi, E. Stavitski, J. Gascon, F. Kapteijn, G.V. Baron, J.F.M. Denayer, ChemSusChem 15 (2012) 740–750.
[8] L.J. Murray, M. Dinca, J.R. Long, Chem. Soc. Rev. 38 (2009) 1294–1314.
[9] J.R. Li, R.J. Kuppler, H.C. Zhou, Chem. Soc. Rev. 38 (2009) 1477–1504.
[10] L. Hamon, P.L. Llewellyn, T. Devic, A. Ghoufi, G. Clet, V. Guillerm, G.D. Pirngruber, G. Maurin, C. Serre, G. Driver, W. Van Beek, E. Jolimaitre, A. Vimont, M. Daturi, G. Férey, J. Am. Chem. Soc. 131 (2009) 17490–17499.
[11] L. Ma, J.M. Falkowski, C. Abney, W. Lin, Nat. Chem. 2 (2010) 838–846.
[12] J. Lee, O.K. Farha, J. Roberts, K.A. Scheidt, S.T. Nguyen, J.T. Hupp, Chem. Soc. Rev. 38 (2009) 1450–1459.
[13] K. Manna, T. Zhang, M. Carboni, C.W. Abney, W. Lin, J. Am. Chem. Soc. 136 (2012) 13182–13185.
[14] L.E. Kreno, K. Leong, O.K. Farha, M. Allendorf, R.P.V. Duyne, J.T. Hupp, Chem. Rev. 112 (2012) 1105–1125.
[15] K. Müller-Buschbaum, F. Beuerle, C. Feldmann, Microporous Mesoporous Mater. 216 (2015) 171–199.
[16] Z. Hu, B.J. Deibert, J. Li, Chem. Soc. Rev. 43 (2014) 5815–5840.
[17] M.D. Allendorf, C.A. Bauer, R.K. Bhakta, R.J.T. Houk, Chem. Soc. Rev. 38 (2009) 1330–1352.
[18] Y. Cui, Y. Yue, G. Qian, B. Chen, Chem. Rev. 112 (2012) 1126–1162.
[19] Y. Cui, B. Chen, G. Qian, Coord. Chem. Rev. 273–274 (2014) 76–86.
[20] D. Liu, C. Poon, K. Lu, C. He, W. Lin, Nat. Commun. 5 (2014) 4182–4192.
[21] K.M.L. Taylor-Pashow, J.D. Rocca, Z.G. Xie, S. Tran, W. Lin, J. Am. Chem. Soc. 131 (2009) 14261–14263.
[22] P. Horcajada, T. Chalati, C. Serre, B. Gillet, C. Sebrie, T. Baati, J.F. Eubank, D. Heurtaux, P. Clayette, C. Kreuz, J.S. Chang, Y.K. Hwang, V. Marsaud, Y.-N. Bories, L. Cynober, S. Gil, G. Férey, P. Couvreur, R. Gref, Nat. Mater. 9 (2010) 172–178.
[23] T. Uemura, N. Yanai, S. Kitagawa, Chem. Soc. Rev. 38 (2009) 1228–1236.
[24] M. Eddaoudi, J. Kim, N. Rosi, D. Vodak, J. Wachter, M. O'Keeffe, O.M. Yaghi, Science 295 (2002) 469–472.
[25] S. Biswas, T. Ahnfeldt, N. Stock, Inorg. Chem. 50 (2011) 9518–9526.
[26] S. Biswas, D.E.P. Vanpoucke, T. Verstraelen, M. Vandichel, S. Couck, K. Leus, Y.-Y. Liu, M. Waroquier, V. Van Speybroeck, J.F.M. Denayer, P. Van Der Voort, J. Phys. Chem. C 117 (2013) 22784–22796.
[27] S. Biswas, J. Zhang, Z. Li, Y.-Y. Liu, M. Grzywa, L. Sun, D. Volkmer, P. Van Der Voort, Dalton Trans. 42 (2013).
[28] S. Biswas, P. Van Der Voort, Eur. J. Inorg. Chem. 2013 (2013) 2154–2160.
[29] A. Buragohain, P. Van Der Voort, S. Biswas, Microporous Mesoporous Mater. 215 (2015) 91–97.
[30] A. Buragohain, S. Couck, P. Van Der Voort, J.F.M. Denayer, S. Biswas, J. Solid State Chem. 238 (2016) 195–202.
[31] L.M. Huang, H.T. Wang, J.X. Chen, Z.B. Wang, J.Y. Sun, D.Y. Zhao, Y.S. Yan, Microporous Mesoporous Mater. 58 (2003) 105–114.
[32] J.A. Greathouse, M.D. Allendorf, J. Am. Chem. Soc. 128 (2006) 10678–10679.
[33] Y. Li, R.T. Yang, Langmuir 23 (2007) 12937–12944.
[34] S.S. Kaye, A. Dailly, O.M. Yaghi, J.R. Long, J. Am. Chem. Soc. 129 (2007) 14176–14177.
[35] D. Ma, Y. Li, Z. Li, Chem. Commun. 47 (2011) 7377–7379.
[36] B. Wang, A.P. Cote, H. Furukawa, M. O'Keeffe, O.M. Yaghi, Nature 453 (2008) 207–211.
[37] L. Hamon, E. Jolimaître, G.D. Pirngruber, Ind. Eng. Chem. Res. 49 (2010) 7497–7503.
[38] Y.-S. Bae, B.G. Hauser, O.M. Farha, J.T. Hupp, R.Q. Snurr, Microporous Mesoporous Mater. 141 (2011) 231–235.
[39] S. Keskin, T.M. VanHeest, D.S. Sholl, ChemSusChem 3 (2010) 879–891.
[40] R. Babarao, S. Dai, J. Jiang, Langmuir 27 (2011) 3451–3460.
[41] M. Dan-Hardi, C. Serre, T. Frot, L. Rozes, G. Maurin, C. Sanchez, G. Ferey, J. Am. Chem. Soc. 131 (2009) 10857–10859.
[42] J.H. Cavka, S. Jakobsen, U. Olsbye, N. Guillou, C. Lamberti, S. Bordiga, K.P. Lillerud, J. Am. Chem. Soc. 130 (2008) 13850–13851.
[43] V. Bon, I. Senkovska, M.S. Weiss, S. Kaskel, CrystEngComm 15 (2013) 9572–9577.
[44] Y. Bai, Y. Dou, L.-H. Xie, W. Rutledge, J.-R. Li, H.-C. Zhou, Chem. Soc. Rev. 45 (2016) 2327–2367.
[45] M. Kim, S.M. Cohen, CrystEngComm 14 (2012) 4096–4104.
[46] S. Wang, J. Wang, W. Cheng, X. Yang, Z. Zhang, Y. Xu, H. Liu, Y. Wu, M. Fang, Dalton Trans. 44 (2015) 8049–8061.
[47] Q. Yang, H. Jobic, F. Salles, D. Kolokolov, V. Guillerm, C. Serre, G. Maurin, Chem. Eur. J. 17 (2011) 8882–8889.
[48] Q. Yang, A.D. Wiersum, H. Jobic, V. Guillerm, C. Serre, P.L. Llewellyn, G. Maurin, J. Phys. Chem. C 115 (2011) 13768–13774.
[49] W. Zhang, H. Huang, D. Liu, Q. Yang, Y. Xiao, Q. Ma, C. Zhong, Microporous Mesoporous Mater. 171 (2013) 118–124.
[50] V. Guillerm, F. Ragon, M. Dan-Hardi, T. Devic, M. Vishnuvarthan, B. Campo, A. Vimont, G. Clet, Q. Yang, G. Maurin, G. Férey, A. Vittadini, S. Gross, C. Serre, Angew. Chem. Int. Ed. 51 (2012) 9267–9271.
[51] M. Lammert, M.T. Wharmby, S. Smolders, B. Bueken, A. Lieb, K.A. Lomachenko, D.D. Vos, N. Stock, Chem. Commun. 51 (2015) 12578–12581.
[52] A. Buragohain, S. Biswas, CrystEngComm 18 (2016) 4374–4381.
[53] F. Xu, H. Wang, S.J. Teat, W. Liu, Q. Xia, Z. Li, J. Li, Dalton Trans. 44 (2015) 20459–20463.
[54] M.-J. Dong, M. Zhao, S. Ou, C. Zou, C.-D. Wu, Angew. Chem. Int. Ed. 53 (2014) 1575–1579.
[55] H. Kumagai, Y. Oka, K. Inoue, M. Kurmoo, 2002, J. Chem. Soc. Dalton Trans. (2002) 3442–3446.
[56] T.K. Prasad, M.P. Suh, Chem. Eur. J. 18 (2012) 8673–8680.
[57] B. Wu, Z.-G. Ren, H.-X. Li, M. Dai, D.-X. Li, Y. Zhang, J.-P. Lang, Inorg. Chem. Commun. 12 (2009) 1168–1170.
[58] A. Modrow, M. Feyand, D. Zargarani, R. Herges, N. Stock, Z. Anorg, Allg. Chem. 638 (2012) 2138–2143.
[59] M. Xue, S. Ma, Z. Jin, R.M. Schaffino, G.-S. Zhu, E.B. Lobkovsky, S.-L. Qiu, B. Chen, Inorg. Chem. 47 (2008) 6825–6828.
[60] V. Petricek, M. Dusek, L. Palatinus, Jana2000 – The Crystallographic Computing System Institute of Physics, Czech Republic, Praha, 2000.
[61] A.K. Rappe, C.J. Casewit, K.S. Colwell, W.A. Goddard III, W.M. Skiff, J. Am. Chem. Soc. 114 (1992) 10024–10035.
[62] C.J. Casewit, K.S. Colwell, A.K. Rappe, J. Am. Chem. Soc. 114 (1992) 10035–10046.
[63] C.J. Casewit, K.S. Colwell, A.K. Rappe, J. Am. Chem. Soc. 114 (1992) 10046–10053.
[64] A.K. Rappe, K.S. Colwell, C.J. Casewit, Inorg. Chem. 32 (1993) 3438–3450.
[65] N. Stock, S. Biswas, Chem. Rev. 112 (2012) 933–969.
[66] C.N. Banwell, E.M. McCash, Fundamentals of Molecular Spectroscopy, McGraw Hill, New York, 1994.
[67] J.H. Cavka, C.A. Grande, G. Mondino, R. Blom, Ind. Eng. Chem. Res. 53 (2014) 15500–15507.
[68] M. SK, M. Grzywa, D. Volkmer, S. Biswas, J. Solid State Chem. 232 (2015) 221–227.
[69] M. SK, S. Bhowal, S. Biswas, 2015, Eur. J. Inorg. Chem. (2015) 3317–3322.
[70] M. SK, S. Biswas, CrystEngComm 18 (2016) 3104–3113.
[71] G.C. Shearer, S. Chavan, S. Bordiga, S. Svelle, U. Olsbye, K.P. Lillerud, Chem. Mater. 28 (2016) 3749–3761.
[72] R.C. Klet, Y. Liu, T.C. Wang, J.T. Hupp, O.K. Farha, J. Mater. Chem. A 4 (2016) 1479–1485.
[73] G.C. Shearer, S. Chavan, J. Ethiraj, J.G. Vitillo, S. Svelle, U. Olsbye, C. Lamberti, S. Bordiga, K.P. Lillerud, Chem. Mater. 26 (2014) 4068–4071.
[74] H. Wu, Y.S. Chua, V. Krungleviciute, M. Tyagi, P. Chen, T. Yildirim, W. Zhou, J. Am. Chem. Soc. 135 (2013) 10525–10532.
[75] L. Sarkisov, A. Harrison, Mol. Simul. 37 (2011) 1248–1257.